

Mixed-Ligand Complexes of Ruthenium(II): Factors Governing Binding to DNA

A. M. Pyle, J. P. Rehmman, R. Meshoyrer, C. V. Kumar,[†] N. J. Turro,* and J. K. Barton*

Contribution from the Department of Chemistry, Columbia University, New York, New York 10027. Received August 4, 1988

Abstract: Binding and spectroscopic parameters for a series of mixed-ligand complexes on binding to DNA have been determined. The application of mixed-ligand complexes permits the variation in geometry, size, hydrophobicity, and hydrogen-bonding ability by systematic variation of complex ligands and the determination of how these factors contribute to DNA binding affinity. Ligands employed include 2,2'-bipyridine (bpy), 1,10-phenanthroline (phen), 4,7-diphenylphenanthroline (DIP), 5-nitrophenanthroline (5-NO₂-phen), 4,5-diazafluorene-9-one (flone), and 9,10-phenanthrenequinonediimine (phi). Measurements include equilibrium binding isotherms and enantioselectivities associated with binding, the degree of absorption hypochromism and red shift in the ruthenium charge-transfer band, increases in emission intensities and excited-state lifetimes, perturbations in excited-state resonance Raman spectra (which reflect changes in excited-state charge-transfer distributions as a result of binding to DNA), and determinations of helical unwinding. The complexes examined, with the exception of Ru(bpy)₃²⁺, all appear to intercalate and surface-bind to DNA, and for those that bind appreciably, enantioselectivity is observed. Based upon the measurements of spectroscopic properties and binding isotherms, the intercalating ability appears to increase over the series bpy ≪ phen ≤ DIP ≪ phi. Correlations between hydrophobicity and DNA binding affinity are observed. The introduction of hydrogen-bonding functionalities provides no net increase in DNA binding affinity. Most critical in determining overall affinity appears to be the shape of the complex and how that shape matches the DNA. The array of well-defined shapes and structures, conveniently prepared and varied for these mixed-ligand complexes, coupled with the spectroscopic handle available by monitoring perturbations in the charge-transfer state of the ruthenium(II) complexes, can be useful in systematic studies of DNA recognition as well as that of other biopolymers.

There has been considerable interest in elucidating those factors that determine affinity and selectivity in binding of small molecules to DNA.¹⁻⁷ A quantitative understanding of such factors that determine recognition of DNA sites would be valuable in the rational design of sequence-specific DNA binding molecules for application in chemotherapy and in the development of tools for biotechnology. Much work has focused on the elucidation of noncovalent interactions with DNA by small natural products and their synthetic derivatives.²⁻⁷ These small molecules are stabilized in binding to DNA through a series of weak interactions, such as the π -stacking interactions associated with intercalation of aromatic heterocyclic groups between the base pairs, and hydrogen-bonding and van der Waals interactions of functionalities bound along the groove of the DNA helix. It would be valuable to understand quantitatively the contributions from these different modes to stabilization of the bound complex at a DNA site.

In our laboratories we have focused on the examination of noncovalent interactions with DNA of transition-metal complexes of phenanthroline.^{1,8-11} The cationic complexes have been found both to intercalate into DNA and to bind noncovalently in a surface-bound or groove-bound fashion. These interactions with DNA have been characterized largely through spectroscopic and photophysical studies, and determinations of enantiomeric selectivities associated with binding by the metal complexes have been helpful also in establishing models.^{8,9} On the basis of these investigations, intercalation likely occurs preferentially from the major groove of the DNA helix and is favored for the Δ isomer into a right-handed helix. In the case of the surface-bound interaction, it likely occurs along the minor groove of the helix and it is the Λ isomer that is favored in surface-binding to right-handed DNA helices. Figure 1 illustrates our models for these binding interactions.

Based upon these binding interactions, derivatives of tris(phenanthroline) complexes have been developed that recognize selectively different conformations of DNA. By matching shapes and symmetries of the metal complexes to those of DNA conformations, probes for A and Z DNA have been designed.¹⁰ Most recently, a diphenylphenanthroline complex of rhodium(III) has

been found to induce double-stranded cleavage at cruciform sites upon photoactivation.¹¹ Although these complexes lack hydrogen-bonding donors and acceptors and therefore must be associating with the DNA only through a mixture of van der Waals and intercalative interactions, a high level of specificity is associated with the recognition of different DNA sites by these complexes. It becomes important, therefore, to begin to establish the contributions of these weak interactions to binding stability and selectivity.

In this report we explore the interactions of mixed-ligand complexes of ruthenium(II) with B DNA using a variety of biophysical and spectroscopic methods. Ruthenium(II) complexes of phenanthroline, phenanthrenequinonediimine, and derivatives thereof are extremely useful for the construction and characterization of DNA binding molecules owing to their intense optical

(1) Barton, J. K. *Science* **1986**, *233*, 727.

(2) Dervan, P. B. *Science* **1986**, *232*, 464. Wade, W. S.; Dervan, P. B. *J. Am. Chem. Soc.* **1987**, *109*, 1574.

(3) Berman, H. M.; Young, P. R. *Annu. Rev. Biophys. Bioeng.* **1981**, *10*, 87.

(4) Waring, M. J.; Fox, K. R.; Grigg, G. W. *Biochem. J.* **1987**, *143*, 847. Burckhardt, G.; Waehnert, U.; Luck, G.; Zimmer, C. *Stud. Biophys.* **1986**, *114*, 225. Kissinger, K.; Krowicki, K.; Dabrowiak, J. C.; Lown, J. W. *Biochemistry* **1987**, *26*, 5590.

(5) Quigley, G. J.; Ughetto, G.; van der Marel, G.; van Boom, J. H.; Wang, A. H.-J.; Rich, A. *Science* **1986**, *232*, 1255. Kopka, M. L.; Yoon, C.; Goodsell, D.; Pjura, P.; Dickerson, R. E. *Proc. Natl. Acad. Sci. U.S.A.* **1985**, *82*, 1376. Pjura, P. E.; Grzeskowiak, K.; Dickerson, R. E. *J. Mol. Biol.* **1987**, *197*, 257.

(6) Wilson, W. D.; Wang, Y.-H.; Kusuma, S.; Chandrasekaran, S.; Yang, N. C.; Boykin, D. W. *J. Am. Chem. Soc.* **1985**, *107*, 4989.

(7) Breslauer, K. J.; Remata, D. P.; Chou, W. Y.; Ferrante, R.; Curry, J.; Zaunczkowski, D.; Snyder, J. G.; Marky, L. A. *Proc. Natl. Acad. Sci. U.S.A.* **1987**, *84*, 8922. Ibanez, V.; Geacintov, N. E.; Gagliano, A. G.; Brondimarte, S.; Harvey, R. G. *J. Am. Chem. Soc.* **1980**, *102*, 5661.

(8) Kumar, C. V.; Barton, J. K.; Turro, N. J. *J. Am. Chem. Soc.* **1985**, *107*, 5518.

(9) Barton, J. K.; Goldberg, J. M.; Kumar, C. V.; Turro, N. J. *J. Am. Chem. Soc.* **1986**, *108*, 2081. J. Rehmman Ph.D. Dissertation, Columbia University.

(10) Mei, H.-Y.; Barton, J. K. *Proc. Natl. Acad. Sci. U.S.A.* **1988**, *85*, 1339. Barton, J. K.; Raphael, A. L. *Proc. Natl. Acad. Sci. U.S.A.* **1985**, *82*, 6460.

(11) Kirshenbaum, M. R.; Tribolet, R.; Barton, J. K. *Nucleic Acids Res.* **1988**, *16*, 7943.

[†] Present address: Department of Chemistry, Box U-60, University of Connecticut, Storrs, CT, 06269.

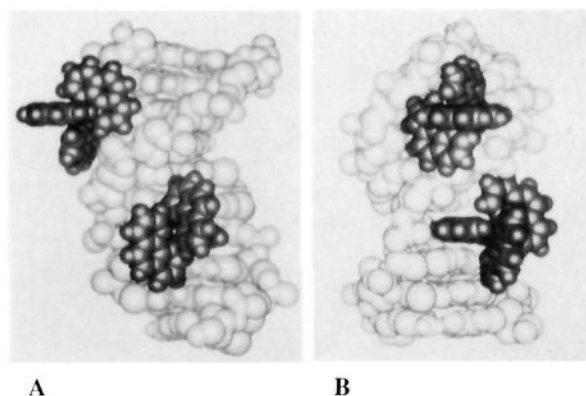


Figure 1. Models for the two noncovalent binding interactions of the octahedral metal complexes with DNA. Shown are Δ -Ru(phen)₃²⁺ (bottom) intercalated into the major groove and Λ -Ru(phen)₃²⁺ (top) surface-bound against the minor groove of the DNA helix. Figure B displays the same models after a 90° rotation about the helical axis. Graphics were performed on an Evans and Sutherland PS390 terminal using the MACROMODEL program.

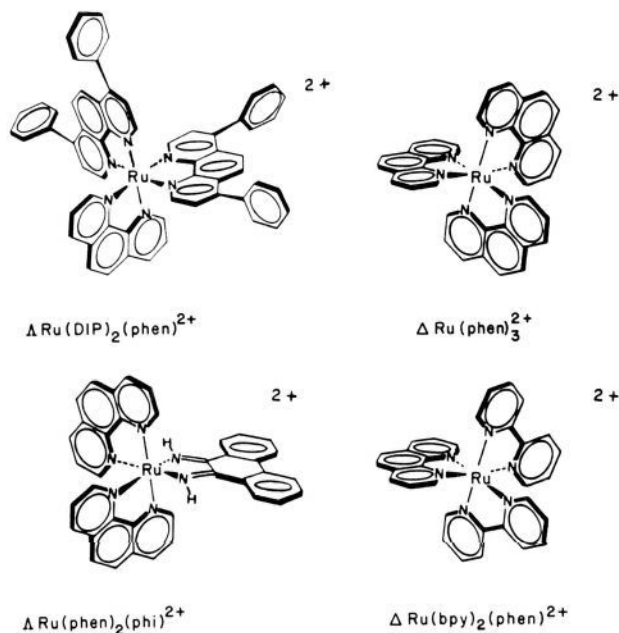


Figure 2. Illustrations of several mixed-ligand complexes: Λ -Ru(DIP)₂(phen)²⁺ (top left); Δ -Ru(phen)₃²⁺ (top right); Λ -Ru(phen)₂(phi)²⁺ (bottom left); Δ -Ru(bpy)₂(phen)²⁺ (bottom right).

absorption and emission, their relative ease of preparation, and their inertness to substitution and racemization.¹²⁻¹⁴ A subset of the complexes being examined is shown schematically in Figure 2. The complexes examined are coordinatively saturated and rigid in structure. All are dications and therefore the electrostatic component of the binding is a constant across the series (to first approximation given some size variation). By varying ligands and ligand substituents in the complexes in a systematic fashion, as illustrated in Figure 2, and comparing binding parameters for the series, we may determine the contributions of the different ligand functionalities and sizes to the binding interactions with DNA. The ligands employed in this study are given in Figure 3. The study of the mixed-ligand complexes with DNA offers the opportunity to explore systematically how such factors as molecular shape and hydrogen bonding stabilize small molecules on DNA.

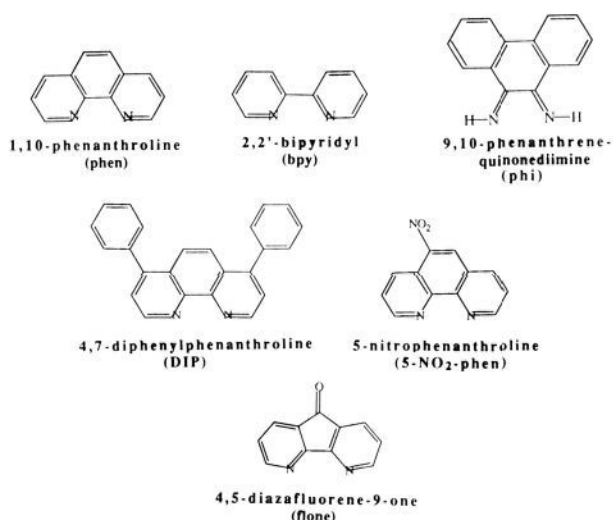


Figure 3. Ligands used for the synthesis of mixed-ligand ruthenium complexes.

Experimental Section

Synthesis and Characterization. Materials. RuCl₃·3H₂O was purchased from Engelhard Co. Ligands (Aldrich) were checked for purity by NMR and recrystallized if necessary.

[Ru(bpy)₂(phen)]Cl₂, [Ru(phen)₂(bpy)]Cl₂. These complexes were synthesized by methods described previously.¹⁵

[Ru(phen)₂(DIP)]Cl₂. Ru(phen)₂Cl₂ (1 mmol) was added to 1 equiv of 4,7-diphenyl-1,10-phenanthroline (DIP) and refluxed in 14 mL of 75% ethanol/water for 30 min. The product was isolated as the ClO₄⁻ salt for chromatography on cellulose (10% CHCl₃/hexane) and converted to the chloride salt by ion exchange: NMR (DMSO) δ 8.79 (4 dd), 8.4 (4 s), 8.24 (2 d), 8.22 (2 s), 8.16 (2 d), 8.08 (2 d), 7.83 (2 dd), 7.78 (2 dd), 7.75 (2 d), 7.63 (10 m); FABMS ion mass 794 [Ru(phen)₂(DIP)]²⁺, 614 [Ru(phen)(DIP)]²⁺.

[Ru(bpy)₂(DIP)]Cl₂: synthesized as described above, using Ru(bpy)₂Cl₂ rather than Ru(phen)₂Cl₂ as starting material.

[Ru(DIP)₂(phen)]Cl₂. Ru(DIP)₂Cl₂ was refluxed in ethanol with 1 equiv of phenanthroline. The product was purified by cellulose chromatography. The Ru(DIP)₂Cl₂ starting material, like the other bis(polypyridyl) complexes, was readily prepared by dissolving 3 mmol of RuCl₃·3H₂O, 30 mmol of LiCl, and 6 mmol of DIP ligand in 100 mL of DMF and refluxing for 4 h. The reaction mixture was stripped of solvent and the product precipitated from ethanol/water. Further purification was as for [Ru(phen)₂(DIP)]Cl₂: NMR (DMSO) δ 8.82 (2 d), 8.42 (2 s), 8.34 (2 d), 8.25 (4 s), 8.23 (2 d), 8.18 (2 d), 7.87 (2 dd), 7.80 (2 d), 7.74 (2 d), 7.69 (20 m); FABMS ion mass 946 [Ru(DIP)₂(phen)]²⁺, 766 [Ru(DIP)]²⁺, 614 [Ru(DIP)(phen)]²⁺.

[Ru(5-nitrophenanthroline)]₃Cl₂: synthesized as described by Lin et al.¹⁶

[Ru(phen)₂(4,5-diazafluorene-9-one)]Cl₂. One equivalent of 4,5-diazafluorene-9-one and a suspension of 1 mmol of Ru(phen)₂Cl₂ in 30 mL of wet ethanol were refluxed for 4 h and recrystallized from acetone/heptane. The 4,5-diazafluorene-9-one ligand was synthesized as described by Henderson et al.¹⁷ NMR (CD₃CN) δ 8.71 (2 dd), 8.61 (2 dd), 8.55 (2 dd), 8.25 (4 d), 8.10 (2 d), 8.03 (2 dd), 7.88 (2 m), 7.59 (4 m), 7.39 (2 m); FABMS ion mass 644 [Ru(phen)₂(flone)]²⁺.

[Ru(bpy)₂(phi)]Cl₂. This complex was prepared as previously reported by Belser et al.¹³ NMR (DMSO) δ 13.67 (2 s, NH), 8.68 (4 d), 8.60 (2 d), 8.35 (2 d), 8.05 (2 t), 8.0 (2 t), 7.75 (2 d), 7.57 (2 t), 7.43 (8 m); FABMS ion mass 620 [Ru(bpy)₂(phi)]²⁺, 465 [Ru(bpy)(phi)]²⁺, 414 [Ru(bpy)₂]²⁺, 257 [Ru(bpy)]²⁺. Anal. Calcd for [Ru(bpy)₂(phi)](PF₆)₂: C, 44.90; H, 2.90; N, 9.20. Found C, 44.62; H, 3.02; N, 8.9. A crystal structure (data not shown), determined by X-ray diffraction analysis, confirms the coordination geometry of this species.

[Ru(phen)₂(phi)]Cl₂. As with the synthesis of Ru(bpy)₂(phi)Cl₂, this compound was prepared by refluxing 0.19 mmol of Ru(phen)₂Cl₂, 1.2 mL of 0.1 M NaOH, and 0.7 mmol of diaminophenanthrene in 5 mL of H₂O containing a catalytic amount of zinc dust. After 1 h, 3 mL of

(12) Meyer, T. J. *Pure Appl. Chem.* **1986**, *58*, 1193. Sutin, N.; Creutz, C. *Pure Appl. Chem.* **1980**, *52*, 2717.

(13) Belser, P.; von Zelewsky, A.; Zehnder, M. *Inorg. Chem.* **1981**, *20*, 3098.

(14) Pyle, A. M.; Barton, J. K. *Inorg. Chem.* **1987**, *26*, 3820.

(15) Krause, R. A. *Inorg. Chim. Acta* **1977**, *22*, 209.

(16) Lin, C.-T.; Botcher, W.; Chou, M.; Creutz, C.; Sutin, N. *J. Am. Chem. Soc.* **1976**, *98*, 6536.

(17) Henderson, L. J.; Fronczek, F. R.; Cherry, W. R. *J. Am. Chem. Soc.* **1984**, *106*, 5876.

EtOH was added, and the resultant purple solution was air oxidized for 16 h in the presence of 0.5 mL of NH_4OH . The final red solution was extracted with diethyl ether to remove organic impurities and precipitated with KCl: NMR (DMSO) δ 13.81 (2 s, NH), 8.86 (2 d), 8.75 (2 d), 8.63 (2 d), 8.55 (4 m), 8.37 (4 s), 8.05 (1 d), 7.95 (1 d), 7.85 (1 d), 7.80 (2 d), 7.78 (1 d), 7.73 (2 t), 7.57 (2 t); FABMS ion mass 667 $[\text{Ru}(\text{phen})_2(\text{phi})]^{2+}$, 488 $[\text{Ru}(\text{phen})(\text{phi})]^{2+}$, 460 $[\text{Ru}(\text{phen})_2]^{2+}$, 282 $[\text{Ru}(\text{phen})]^{2+}$. Anal. Calcd for $\text{Ru}(\text{phen})_2(\text{phi})\text{Cl}_2 \cdot \text{KCl} \cdot 5\text{H}_2\text{O}$: C, 50.50; H, 4.02; N, 9.30. Found: C, 50.11; H, 4.04; N, 9.84.

$[\text{Ru}(\text{phi})_2(\text{bpy})]\text{Cl}_2$: obtained by a synthesis identical with that for $[\text{Ru}(\text{benzoquinonediimine})_2(\text{bpy})]\text{Cl}_2$.¹³ 9,10-Diaminophenanthrene was used as the ligand substrate instead of diaminobenzene. In addition, solvent for the final air oxidation step of this compound was 50% ethanol/water rather than pure water. Like the other phi-containing compounds, this complex was first isolated as the PF_6^- salt and converted to the chloride by precipitation with KCl or ion exchange on AG MP-1 resin from Bio-Rad: NMR (DMSO) δ 14.16 (2 s, NH), 12.87 (2 s, NH), 8.78 (4 t), 8.6 (2 d), 8.52 (4 d), 8.20 (4 m), 7.75 (4 t), 7.65 (6 m); FABMS ion mass 669 $[\text{Ru}(\text{phi})_2(\text{bpy})]^{2+}$, 514 $[\text{Ru}(\text{phi})_2]^{2+}$, 464 $[\text{Ru}(\text{phi})(\text{bpy})]^{2+}$, 307 $[\text{Ru}(\text{phi})]^{2+}$. Anal. Calcd for $\text{Ru}(\text{phi})_2(\text{bpy})\text{Cl}_2 \cdot 6\text{H}_2\text{O}$: C, 53.78; H, 4.76; N, 9.90. Found: C, 53.84; H, 4.96; N, 9.02.

Methods. Instrumentation. NMR spectra were recorded on a Varian VXR 300-MHz spectrometer. FABMS were performed with a VG Analytical 7070EQ Mass Spectrometer,¹⁸ and elemental analyses were done by Galbraith Laboratories in Nashville, TN. UV-visible absorbance spectra were recorded on a Varian Cary-219 absorbance spectrophotometer. Extinction coefficients for the compounds were determined versus ruthenium concentrations obtained by atomic absorption spectroscopy with known ruthenium standards. $[\text{Ru}(\text{bpy})_3]\text{Cl}_2$ solutions were also employed for these determinations as an internal standard. A Varian AA-875 atomic absorption spectrophotometer was used for these determinations.

Emission spectra were measured on a Perkin-Elmer LS-5 fluorescence spectrometer. The samples were excited at their corresponding isosbestic points. All the measurements were made at 20 °C in a thermostated cuvette holder with 3-nm entrance slit and 10-nm exit slit. Ruthenium solutions employed were 7 μM in concentration and calf thymus DNA was added to a ratio of 40:1 nucleotide/metal; ruthenium-DNA solutions were allowed to incubate for 15 min before enhanced spectra were recorded. The emission enhancement factors were measured by comparing the intensities at the emission spectral maxima in the absence and presence of DNA, under similar conditions.

The luminescence lifetime measurements were done on a PRA SPC (single-photon counting) spectrometer with some minor modifications. The samples were excited with a nitrogen-filled thyratron gated flash lamp and the data were collected with a Tracor Northern 1710 multi-channel analyzer. The data were then transferred to a PDP-11/03 computer and deconvoluted with PRA software. The validity of the convergent biexponential fits was checked using four different tests. A concentrated solution of DNA (5 mM DNA phosphate) in buffer was added to a solution of the metal complex (4 μM) in buffer and allowed to equilibrate. Lifetimes of the samples were measured 0.5 h after the metal complexes were mixed with DNA. All measurements were made at 20 °C and under air-saturated conditions.

Excited-state resonance Raman spectra were run on a home-built Raman spectrometer with an intensified multichannel detector.¹⁹ The samples were excited by a QuantaRay, Q-switched, Nd-YAG laser (DCR-2, FWHM = 6 ns, 5 mJ per pulse at 355 nm). The laser power was high enough to saturate the excited-state population and also to scatter off from the excited state formed during the laser pulse width. The sample solution was pumped through a nozzle to form a smooth thin jet which was intercepted by the laser. The back-scattered light was collected at a small angle to the pump beam and focused onto the entrance slit of the Spex triple-mate spectrograph. The third stage of the spectrograph contained a 2400 grooves/mm grating to provide $\sim 2 \text{ cm}^{-1}$ resolution for the Raman experiments. The entire experiment was run by a homemade menu-driven program with customized graphics written in Heminway Basic. The spectra were calibrated by using the known spectrum of $\text{Ru}(\text{bpy})_3^{2+}$.²⁰ To a solution of calf thymus DNA (1 mM) was added $\text{Ru}(\text{bpy})_2\text{DIP}^{2+}$ (40 μM), and the solution was left to equilibrate for 0.5 h. The solution was then circulated as a thin, smooth and

slow stream. No degradation in the sample, as determined by optical absorption, was observed after recording of the Raman spectrum under these conditions.

Measurement of Solubilities. Solubilities of the compounds were measured by preparing saturated solutions of metal complex in buffer (50 mM NaCl, 5 mM Tris, pH 7.5) and allowing the suspensions to equilibrate for 24 h at 25 °C. After that time, the solutions were spun down in an Eppendorff microcentrifuge at 15000 rpm for 2 min and the supernatant was carefully removed by pipet. After dilution, the ruthenium concentrations were measured by UV-visible absorbance.

Equilibrium Dialysis. Equilibrium dialysis of the racemic metal complexes was performed against calf thymus DNA using procedures described previously.⁹ The buffer used was 5 mM Tris, 50 mM NaCl at pH 7.5. Samples were agitated on a shaker bath during equilibration which occurred after 3–5 days, as determined by control samples containing no DNA. After equilibration, volumes of liquid inside and outside the dialysis bags were determined (approximately 1 and 3 mL, respectively) and circular dichroism of the dialysate was measured on a Jasco J-40 spectropolarimeter. Final ruthenium concentrations inside and outside the bags were measured by visible absorbance. Data analysis was performed on a VAX-780 using nonlinear least-squares analysis.

Topoisomerase Assay. In a typical experiment, pBR322 DNA dimer (0.47 μg , BRL) was incubated at 37 °C for 1 h with 2–4 units of topoisomerase I (from calf thymus, BRL) in reaction mixtures containing 5 mM Tris-HCl, pH 7.2, 50 mM NaCl, 1 mM MgCl_2 , and from 1 to 100 μM ruthenium complex (50-mL total volume). Following incubation, the mixtures were ethanol precipitated (200 mL of ethanol) at -20 °C, centrifuged, and resuspended in 20 mL of buffer (no Mg^{2+}). The samples were then electrophoresed in 1% agarose for 4–6 h. Photographic negatives of the agarose gels were scanned on an LKB Model 2202 ultrascan laser densitometer. The unwinding angles were determined graphically from plots of $-\tau$, where τ equals the number of superhelical turns, versus the concentration of bound ruthenium complex, as described by Keller,²¹ by the following equation:²²

$$\sigma = -2r_c(\Phi/360) = -r_c\Phi/18$$

where σ is the superhelical density of the plasmid, r_c is the amount of metal complex ions bound per nucleotide when all of the superhelices are removed, and Φ is the unwinding angle. Bound concentrations were determined by interpolation from the Scatchard plots of equilibrium dialysis data.

Results

Equilibrium Dialysis. Equilibrium binding constants for the metal complexes with DNA may be determined classically by equilibrium dialysis. Calf thymus DNA was dialyzed against the series of mixed-ligand complexes by using a broad range of ruthenium concentrations. Data are shown in Figure 4 for the eight complexes which showed noncooperative binding to the polynucleotide. The results have been plotted according to Scatchard,²³ where r is the ratio of bound metal to DNA phosphate concentration, and c_f is the concentration of free metal complex. The data were fit by nonlinear least-squares analysis to the McGhee and von Hippel equation²⁴ governing random noncooperative binding to a lattice:

$$2r/c_f = K_b(1 - 2lr)[(1 - 2lr)/\{1 - 2(l - 1)r\}]^{-1}$$

where r is the ratio of bound concentration of ruthenium to the concentration of DNA phosphate, c_f is the concentration of ruthenium free in solution, K_b is the intrinsic binding constant, and the integer l , which measures the degree of anticooperativity, is a measure of the thermodynamic site size averaged over all possible sequences on the helix. The curves shown reflect the best fit after variation of two parameters: the intrinsic binding constant, K_b , and binding site size, l . For those complexes where cooperativity was observed, the equation²⁴ incorporating a cooperativity parameter was used. The values obtained are summarized in Table I.

For the complexes shown, the intrinsic binding constant is seen to vary over more than 2 orders of magnitude. The highest binding affinity is seen for complexes that contain the phi ligand. Other

(18) Mass spectral data are reported as mass/ion values, rather than mass/charge ratios.

(19) Kumar, C. V.; Barton, J. K.; Turro, N. J. *Inorg. Chem.* **1987**, *26*, 1455.

(20) Dallinger, R. F.; Woodruff, W. H. *J. Am. Chem. Soc.* **1979**, *101*, 4391. Bradley, P. G.; Kress, N.; Hornberger, B. A.; Dallinger, R.; Woodruff, W. H. *J. Am. Chem. Soc.* **1981**, *103*, 7441. Smothers, W. K.; Wrighton, M. S. *J. Am. Chem. Soc.* **1983**, *105*, 1067.

(21) Keller, W. *Proc. Natl. Acad. Sci. U.S.A.* **1975**, *72*, 4876.

(22) Wang, J. C. *J. Mol. Biol.* **1974**, *89*, 783.

(23) Scatchard, G. *Ann. N.Y. Acad. Sci.* **1949**, *51*, 660.

(24) McGhee, J. D.; von Hippel, P. H. *J. Mol. Biol.* **1974**, *86*, 469.

Table I. DNA Binding Parameters for Mixed-Ligand Complexes of Ruthenium(II)

complex	$K_b, M^{-1} \times 10^3$		site size, ^c base pairs	unwinding concn., ^d μM	unwinding angle, ^e deg	enantioselect ^f
	equilib dialysis ^a	absorptn titratn ^b				
Ru(bpy) ₃ Cl ₂	0.7 (0.13)	<i>h</i>	6-12	650		none
Ru(bpy) ₂ (phen)Cl ₂	0.7 (0.07)	<i>h</i>	10-14	69		Δ
Ru(phen) ₂ (bpy)Cl ₂	2.4 (0.4)	4.6 (1.0)	5-7	11	18	Δ
Ru(phen) ₃ Cl ₂	3.1 (0.1)	5.5 (0.99)	4	9	19	Δ
Ru(5-NO ₂ -phen) ₃ Cl ₂	1.0 (0.1)	<i>h</i>	8-12	<i>i</i>		Δ
Ru(phen) ₂ (flone)Cl ₂	2.1 (0.2)	<i>h</i>	9-12	<i>i</i>		none
Ru(bpy) ₂ (DIP)Cl ₂	1.7 (0.3)	<i>h</i>	12-18	170		Δ
Ru(phen) ₂ (DIP)Cl ₂	2.5 (1.0)	11.2 (0.99)	cooperative	9		Δ
Ru(DIP) ₂ (phen)Cl ₂	10.1 (3)	11.1 (0.99)	cooperative	<i>j</i>	<i>j</i>	Δ
Ru(phi) ₂ (bpy)Cl ₂	17.6 (-)	24.4 (0.98)	cooperative	0.6	<i>j</i>	<i>k</i>
Ru(phen) ₂ (phi)Cl ₂	46 (6) ^g	46.8 (0.99)	2-3	1.2	26 ^g	<i>l</i>
	110 (37) ^g					
Ru(bpy) ₂ (phi)Cl ₂	160 (17)	48.0 (0.99)	4	1.1	17	<i>l</i>

^aStandard deviations are given in parentheses. ^bCorrelation coefficients between observed and calculated values are given in parentheses. Values for K_b have been calculated as described in the text. ^cThese values reflect a thermodynamic average binding parameter rather than structurally the size of the molecule bound at any individual site on the helix. For this range of site sizes, less than 1% variation in correlation coefficient and standard deviation in K_b is found. For the lowest site size given, best correlation and the lowest standard deviation in K_b are obtained. For cases of low binding, the values are underestimates. ^dConcentration of ruthenium complex needed to unwind 11 of 22 supercoils. [DNA] = 47 μM for assays of phi-containing complexes and 31.5 μM for all others. ^eUnwinding angles represent the number of degrees by which one molecule of bound complex unwinds the DNA helical duplex. Values are calculated with some certainty only for those complexes where the binding is otherwise well-behaved. ^f Δ 's represent an enantiomeric preference for the Δ isomer in binding to DNA. ^gThe lower binding constant and site size given result from fitting only those points where $r > 0.08$. The higher binding constant given results from inclusion of all points. Although the fit with all points included is poorer, it is probably a better overall estimate of binding affinity. ^hAt the extremely low levels of binding obtained with these complexes, changes in the absorption spectrum were too small to allow for significant determinations. ⁱMeasurements were not conducted on this complex. ^jMeasurement could not be performed due to the poor solubility of the complex. ^kA small circular dichroism was occasionally observed in the dialysate. ^lAlthough the dialysate showed a strong circular dichroism, and thus a clear enantiomeric selectivity in binding to DNA exists, the absolute configurations for the phi complexes cannot be inferred from simple comparison to phenanthroline complexes.

variations, though of a smaller magnitude, are apparent as a function of increasing size and hydrophobicity. For example, for the series Ru(bpy)₃²⁺, Ru(bpy)₂(phen)²⁺, Ru(bpy)₂(DIP)²⁺, and Ru(bpy)₂(phi)²⁺, we find K_b values of 0.7×10^3 , 0.7×10^3 , 1.7×10^3 , and $1.6 \times 10^5 M^{-1}$, respectively. The data for all the complexes fit reasonably well to a random noncooperative model. Site sizes are found to vary between 2 and 12 base pairs, but values obtained for complexes with low binding affinity ($K < 2 \times 10^3 M^{-1}$) have a high associated uncertainty.

The bulkier and more hydrophobic complexes Ru(phen)₂(DIP)²⁺, Ru(DIP)₂(phen)²⁺, and Ru(phi)₂(bpy)²⁺ all showed curves indicative of cooperative binding. This observation is understandable, since these complexes tend to aggregate in solution. Thus the equilibrium involves not only bound and free monomer complexes but those involving self-stacked dimers (or even larger aggregates). Furthermore, a similar aggregation of the complexes along the DNA strands is likely. Some samples actually showed precipitation, and these were not included. The extensive aggregation of Ru(DIP)₃²⁺ and Ru(phi)₃²⁺ completely precluded their incorporation in these studies.

Equilibrium dialysis experiments additionally offer the opportunity to examine any enantiomeric selectivities associated with binding. After dialysis of the DNA against the racemic mixture, optical activity observed in the dialysate reflects an enrichment in the dialysate in the less favored enantiomer. For most of the complexes, optical activity was found in the dialysate. Values for the extent of enantiomeric selectivity could not be quantitated in the absence of determinations of $\Delta\epsilon$ and assignments of absolute configuration. Assuming that the signs of the circular dichroism in the ultraviolet ligand bands are the same for these ligands as that for the parent phenanthroline complex,²⁵ we have assigned the absolute configuration of these complexes by comparison to spectra for enantiomers of Ru(phen)₃²⁺ and have compared levels of enantioselectivity qualitatively through measurements of circular dichroic intensity per ruthenium bound. On the basis of these assumptions, we find enantiomeric selectivities for the polypyridyl complexes to reflect an enrichment in the Δ isomer in the dialysate and the preferential binding of the Δ isomer to the right-handed DNA. This observation is consistent with the preferential intercalation of Δ isomers found earlier for Ru(phen)₃²⁺ and Ru-

(DIP)₃²⁺ in right-handed B DNA.⁸ We may also compare relative enantioselectivities for different ancillary ligands. For the pairs, Ru(phen)₂phi²⁺ versus Ru(bpy)₂phi²⁺, for example, the intensity in circular dichroism per ruthenium bound is more than 3 times greater with phen as the ancillary ligand than with bpy. The same comparison may be seen qualitatively between Ru(phen)₂DIP²⁺ and Ru(bpy)₂DIP²⁺. The exceptions, where no enantiomeric discrimination is apparent, are Ru(phi)₂bpy²⁺, Ru(bpy)₃²⁺, and Ru(phen)₂(flone)²⁺. For Ru(phi)₂bpy²⁺, aggregation of the complex and its poor solubility made the determinations problematic. In the cases of Ru(bpy)₃²⁺ and Ru(phen)₂(flone)²⁺, the low levels of binding and small size of the complex may preclude observation of any selectivity.

Spectroscopic Changes on Binding to DNA. The complexes all possess intense optical absorption owing to their well-characterized metal-to-ligand charge-transfer bands. Furthermore, for all the complexes, this electronic transition is perturbed on binding to DNA. Table II summarizes the spectroscopic properties of the complexes and some of the changes observed.

For those complexes that luminesce, changes in luminescence on DNA binding are found. Increases in emission are apparent with DNA binding, and depending upon the mixed-ligand complex examined, red shifts or blue shifts in the emission spectra are observed (vide infra). As was seen earlier for Ru(phen)₃²⁺ and Ru(DIP)₃²⁺,^{8,9} the decay in emission from the excited ruthenium complex in the presence of DNA is best characterized by a biexponential, with one component having an emission lifetime characteristic of the free ruthenium species, and one longer lived component. For Ru(phen)₃²⁺ and Ru(DIP)₃²⁺, this long-lived component was characterized extensively and found to correspond to emission from the intercalatively bound species; the emission lifetime for the surface-bound species was found to be indistinguishable from the free form. We suggest that the two components may be assigned similarly for these mixed-ligand complexes. Moreover, the similarity in spectroscopic perturbations seen with the mixed-ligand complexes on binding to DNA supports the notion that these complexes also bind to DNA in a similar fashion.

The emission spectra and decay traces therefore suggest that the mixed-ligand complexes all bind to DNA through the mixture of two binding modes: intercalation and surface binding. The emission enhancements provide some gauge of the extent of intercalation as well as binding affinity. After corrections for the differing affinities of phen and DIP mixed-ligand complexes, it

Table II. Spectroscopic Properties on Binding to DNA

complex	absorptn λ_{\max} , nm			emissn λ_{\max} , nm			ϵ_{free} , $\text{M}^{-1} \text{cm}^{-1}$	emissn enhanc, I/I_0	emissn lifetime, ns	
	free	bound	$\Delta\lambda$	free	bound	$\Delta\lambda$			free	bound ^d
Ru(bpy) ₃ ²⁺	450	450	0	615	618	3	14 600	1.06	420	
Ru(bpy) ₂ (phen) ²⁺	452	452	0	611	602	-9	16 000	1.12	450	430 ± 30 (1) 2100 ± 300 (2)
Ru(phen) ₂ (bpy) ²⁺	446	448	2	608	604	-4	19 200	1.43	555	530 ± 30 (1) 2100 ± 260 (2)
Ru(phen) ₃ ²⁺	443	445	2	591	593	2	20 000	1.87	530	630 ± 70 (1) 2300 ± 620 (2)
Ru(5-NO ₂ -phen) ₃ ²⁺	450	454	4	<i>b</i>			20 000 ^c			
Ru(phen) ₂ (flone) ²⁺	436	436	0	<i>b</i>			18 800			
Ru(bpy) ₂ (DIP) ²⁺	454	454	0	615	621	6	18 600	1.13	700	640 ± 40 (1) 4700 ± 600 (2)
Ru(phen) ₂ (DIP) ²⁺	427 ^a	432	5	614	606	-8	20 550	2.06	970	1160 ± 30 (1) 5290 ± 80 (2)
Ru(DIP) ₂ (phen) ²⁺	433	439	6	616	621	+5	29 400	2.14	990	1160 ± 40 (1) 5100 ± 430 (2)
Ru(phi) ₂ (bpy) ²⁺	572	582	10	<i>b</i>			75 300			
Ru(phen) ₂ (phi) ²⁺	535	544	9	<i>b</i>			51 900			
Ru(bpy) ₂ (phi) ²⁺	535	548	13	<i>b</i>			48 000			

^aThe double-humped charge-transfer bands characteristic of ruthenium polypyridyl complexes are such that the higher energy band of Ru(phen)₂(DIP)²⁺ and Ru(DIP)₂(phen)²⁺ is the more intense and is therefore defined as the λ_{\max} of the complex. ^bNonemissive complexes. ^cRu(bpy)₂(phi)²⁺ was previously reported¹³ to luminesce at 620 nm, but in our hands this was found to be due to Ru(bpy)₃²⁺ contamination. ^dExtinction coefficient for Ru(5-NO₂-phen)₃²⁺ was taken from ref 15. ^d(1) and (2) denote first and second components of emission lifetime decay.

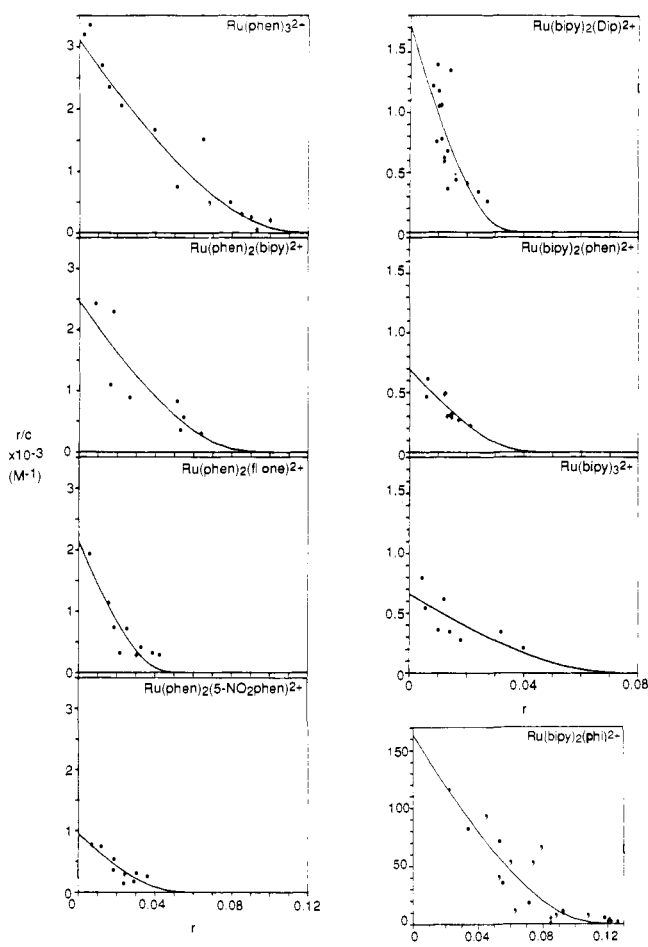


Figure 4. Representative Scatchard plots of binding isotherms for mixed-ligand complexes of ruthenium(II) with calf thymus DNA in buffer at 22 °C, where r is the ratio of bound ruthenium to nucleotide concentrations and C is the concentration of free ruthenium. The solid lines are the best fits to the McGhee and von Hippel equation²⁴ governing noncooperative binding to the helix.

appears from these data that the intercalative component is actually quite comparable among the series. Quantitation of the surface versus intercalative components could not be made, however.

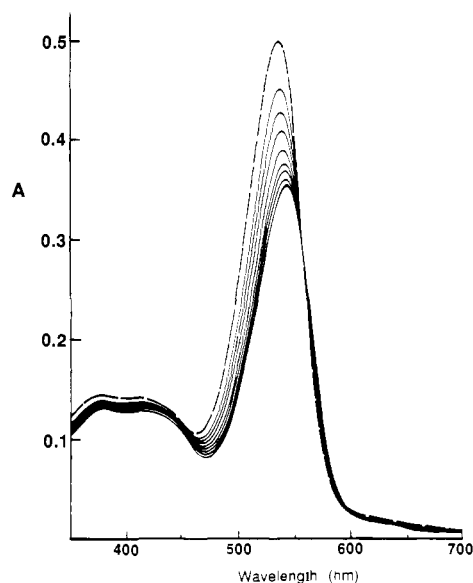


Figure 5. Visible absorption spectra of Ru(phen)₂(phi)²⁺ (10 μM) in the absence (---) and presence (—) of increasing amounts of DNA (0.56 nucleotides/metal per scan).

The binding of intercalative drugs to DNA has also been characterized classically through absorption titrations, following the hypochromism and red shift associated with binding of the colored complex to the helix.²⁶ Figure 5 displays a well-behaved titration of Ru(phen)₂(phi)²⁺ with calf thymus DNA. Isosbestic points are observed at 558 and 598 nm. The spectra show clearly that addition of DNA yields hypochromism and a large red shift in the charge-transfer band of the complex. These spectral characteristics are attributable to a mode of binding that involves a strong stacking interaction between an aromatic chromophore and the base pairs of DNA.

The magnitudes of the red shift and hypochromism are furthermore commonly found to correlate with the strength of the intercalative interaction.²⁶ A comparison of red shifts found with DNA binding can be seen in Table II. Complexes containing phi have the largest red shifts (≤13 nm), followed by DIP complexes (≤6 nm), phen complexes (≤2 nm), and bpy complexes (no red shift). Thus, if red shifts upon binding are taken as a measure

(26) Bloomfield, V. A.; Crothers, D. M.; Tinoco, I., Jr. *Physical Chemistry of Nucleic Acids*; Harper and Row: New York, 1974; p 432.

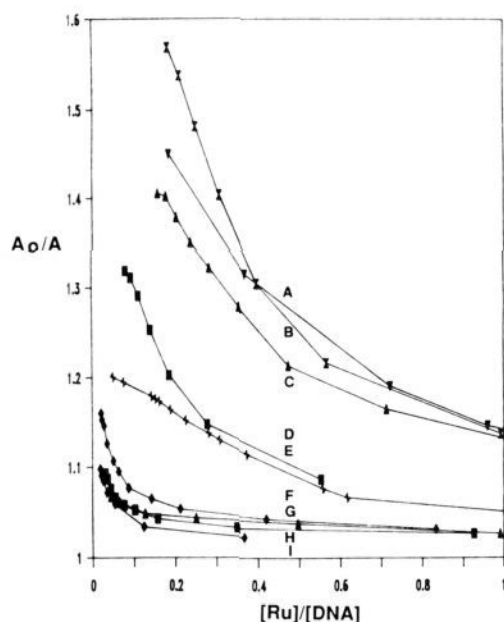


Figure 6. Hypochromism in the visible charge-transfer band as a function of $[Ru]/[DNA]$. A_0/A represents the ratio of absorbance of free ruthenium (in the absence of DNA) to the absorbance as a function of increasing concentrations of added DNA. A, $Ru(DIP)_2(phen)_2^{2+}$; B, $Ru(phen)_2(bpy)_2^{2+}$; C, $Ru(phen)_2(phi)_2^{2+}$; D, $Ru(bpy)_2(phi)_2^{2+}$; E, $Ru(phen)_2(DIP)_2^{2+}$; F, $Ru(phen)_3^{2+}$; G, $Ru(5-NO_2-phen)_3^{2+}$; H, $Ru(phen)_2(flone)_2^{2+}$; I, $Ru(phen)_2(bpy)_2^{2+}$.

of stacking interaction, a trend can be observed in which the optimal shape for intercalation is $\phi > DIP > phen > bpy$.

The degree of hypochromism generally correlates well also with overall binding strength. Figure 6 shows absorption titration data for the series of complexes as a function of DNA addition. The extent of hypochromicity in the charge-transfer band as a function of DNA binding, plotted reciprocally as A_0/A versus $[Ru]/[DNA]$, is found to provide a good measure of relative binding affinity, since the hypochromicity found for the series of complexes per DNA added parallels nicely the binding results by equilibrium dialysis. $Ru(bpy)_2(phi)_2^{2+}$, a soluble complex of high binding strength to DNA, and the more hydrophobic complexes $Ru(phen)_2(DIP)_2^{2+}$, $Ru(DIP)_2(phen)_2^{2+}$, and $Ru(phi)_2(bpy)_2^{2+}$ show the greatest change in absorption with DNA addition. The latter three complexes, however, are only sparingly soluble in the buffer solution and may show increased hypochromism owing to aggregation, both in solution and bound to the helix. Complexes that bind only weakly to DNA, such as $Ru(bpy)_3^{2+}$ and $Ru(bpy)_2(phen)_2^{2+}$, are seen to show little hypochromic effect.

Determinations of intrinsic binding constant, K_b , based upon these absorption titrations may be made with the following equation:²⁷

$$[DNA]/(\epsilon_A - \epsilon_F) = [DNA]/(\epsilon_B - \epsilon_F) + 1/K_b(\epsilon_B - \epsilon_F)$$

where ϵ_A , ϵ_F , and ϵ_B correspond to $A_{obsd}/[Ru]$, the extinction coefficient for the free ruthenium complex, and the extinction coefficient for the ruthenium complex in the fully bound form, respectively. In plots of $[DNA]/(\epsilon_A - \epsilon_F)$ versus $[DNA]$, K_b is given by the ratio of the slope to intercept. This half-reciprocal absorption titration method, which has been used successfully to determine the intrinsic K_b of molecules as hydrophobic as benzol[a]pyrene derivatives,²⁷ was found to provide a useful route to obtain intrinsic binding constants for the broad range of ruthenium complexes of differing solubilities. Values for K_b , given in Table I, were obtained for all but those complexes that bound very weakly; the compounds $Ru(bpy)_3^{2+}$, $Ru(bpy)_2(phen)_2^{2+}$, $Ru(bpy)_2(DIP)_2^{2+}$, $Ru(5-NO_2-phen)_3$, and $Ru(phen)_2(flone)_2^{2+}$ showed such small changes in their absorption spectra upon DNA addition

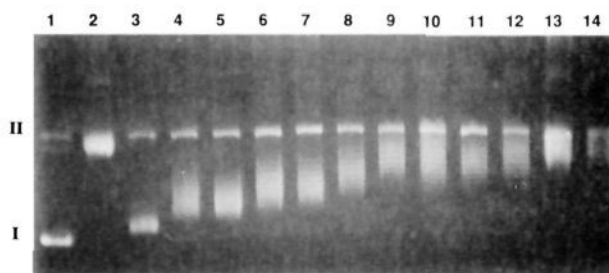


Figure 7. Unwinding of pBR322 DNA by $Ru(bpy)_2(phi)_2^{2+}$ after incubation with topoisomerase I in the presence of increasing concentrations of ruthenium complex as described in the Experimental Section. Lane 1 is DNA control, Lane 2 is DNA and topoisomerase alone, Lanes 3–14 are DNA, topoisomerase, and decreasing Ru concentrations from 5.74 to 1.57 μM . I and II denote forms I and II DNA.

that the resultant error in $\epsilon_A - \epsilon_F$ was large. For the remainder, as shown in Table I, good correlation with those values obtained by dialysis was found.

Unwinding of Supercoiled DNA. The amount of helical unwinding induced by a complex bound to closed circular DNA provides another measure of intercalative binding.^{22,28} Helix unwinding by a noncovalently bound species is determined by observing the change in superhelical density in a plasmid, after relaxation of the plasmid in the presence of bound complex by topoisomerase I and then removal of the complex. The helix unwinding angle is defined as the number of degrees of base pair unwinding per complex bound (see Experimental Section). Figure 7 shows the change in superhelical density of pBR322 DNA dimer after incubation with increasing concentrations of $Ru(bpy)_2(phi)_2^{2+}$ in the presence of topoisomerase. Table I includes both the concentration of ruthenium complex added to unwind the plasmid 50% (11 out of 22 supercoils removed) and, for those complexes that show well-behaved binding parameters, the corresponding unwinding angle per complex bound.

Several trends are apparent from these data. First, those complexes with appreciable binding affinity show reasonable values for the unwinding consistent with intercalation. $Ru(phen)_2^{2+}$ and $Ru(phen)_2(phi)_2^{2+}$ display unwinding angles of 19° and 26°, respectively, and these may be compared to that of 26°, found for ethidium,²² a classical DNA intercalator. For the complexes that bind with lower overall binding strength, unwinding angles could not be reliably determined. The data indicate, however, the inverse correlation between binding constant and concentration of complex required for a constant amount of unwinding. Therefore, it is likely that, for this series of weaker binding molecules, the unwinding angle per complex bound is quite similar. It is noteworthy that bound concentrations reflect both intercalation and surface binding, and thus if surface binding contributes little to the unwinding, those complexes with a greater percentage in the surface-bound form will show reduced apparent unwinding angles. $Ru(bpy)_3^{2+}$, which based upon spectroscopic results neither intercalates nor surface binds to the helix, shows little significant unwinding of the helix. The complexes $Ru(DIP)_2(phen)_2^{2+}$ and $Ru(phi)_2(bpy)_2^{2+}$ proved to be too insoluble for application of the unwinding assay. For the complexes possessing high binding affinity, a larger certainty in bound concentration and therefore unwinding angle exists. Here some effect of the ancillary ligand may be seen. $Ru(phen)_2(phi)_2^{2+}$ exhibits a somewhat greater unwinding angle than $Ru(bpy)_2(phi)_2^{2+}$, suggesting that the larger ancillary phen ligands may contribute to unwinding of the helix.

Effects of DNA Binding Seen by Excited-State Resonance Raman Spectroscopy. The effects of DNA binding on the electronic structure of the complexes may also be probed by excited-state resonance Raman spectroscopy, and this technique has provided some novel evidence in support of intercalative binding.

(28) Waring, M. J. *J. Mol. Biol.* **1970**, *54*, 247.

(29) The unwinding angle for $Ru(phen)_3^{2+}$ has been measured by others as well and compares favorably with our determination. See: Kelly, J. M.; Tossi, A. B.; McConnell, D. J.; OhVigin, C. *Nucleic Acids Res.* **1985**, *13*, 6017.

(27) Wolfe, A.; Shimer, G. H.; Meehan, T. *Biochemistry* **1987**, *26*, 6392.

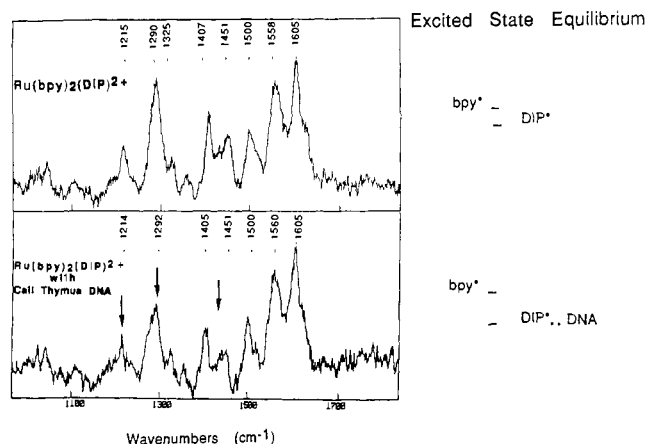


Figure 8. Excited-state resonance Raman spectrum of $\text{Ru}(\text{bpy})_2\text{DIP}^{2+}$ in the absence (top) and presence (bottom) of calf thymus DNA. The arrows indicate those transitions determined earlier³⁰ to reflect excited-state charge transfer which is localized onto the bpy ligand. These spectra indicate that in the presence of DNA the intensity of transitions dominated by charge localization onto bpy is reduced relative to those dominated by charge transfer to the DIP ligand.

Figure 8 shows spectra for $\text{Ru}(\text{bpy})_2\text{DIP}^{2+}$ in the absence and presence of DNA. In the spectra of mixed-ligand complexes, transitions were assigned earlier to excited states localized either on bpy or DIP.³⁰ Thus, the presence of an equilibrium between the two localized excited states was established. In particular, the transitions centered at 1215 and 1290 cm^{-1} are dominated by bpy^* . This equilibrium can be shifted on binding to DNA. In the presence of DNA, the intensity of the transitions corresponding to bpy^* are decreased relative to those for DIP^* . Remarkably, though not covalently bound, the association with DNA sufficiently perturbs the excited-state electronic structure of the complex for detection by this technique. We interpret this decrease in bpy^* transitions relative to DIP^* to reflect the shift in excited-state equilibrium toward DIP^* . For this mixed-ligand complex, only the DIP ligand, rather than bpy, is expected to intercalate into the helix. Perhaps as a result of binding to DNA, the energy of DIP^* is lowered more so than is bpy^* , with charge transfer occurring preferentially onto the intercalated DIP ligand.

One may also understand the red and blue shifts in emission associated with binding to DNA by the mixed-ligand complexes by considering these shifts in equilibria. For $\text{Ru}(\text{bpy})_2\text{DIP}^{2+}$, the lower energy excited state involves transfer to the DIP ligand.³⁰ If DIP is the intercalating ligand, this state is lowered in energy, and consistent with this idea, a red shift (6 nm) in emission is observed. In the case of $\text{Ru}(\text{bpy})_2\text{phen}^{2+}$, the lower energy excited state involves charge transfer onto the bpy ligand.³⁰ Since the phen ligand is the one that would intercalate and thus be lowered in energy, an overall blue shift of 9 nm is observed. The same arguments may explain the shifts observed for $\text{Ru}(\text{phen})_2\text{bpy}^{2+}$ and $\text{Ru}(\text{DIP})_2\text{phen}^{2+}$. For $\text{Ru}(\text{phen})_2\text{DIP}^{2+}$ the direction of the shift found is unexpected, but this may reflect underlying contributions from surface binding.

Discussion

The results of these varied experiments on the series of mixed-ligand complexes of ruthenium(II), when taken together, provide a detailed picture of factors affecting noncovalent binding of the complexes to the helix. The complexes, excepting $\text{Ru}(\text{bpy})_3^{2+}$, all appear to intercalate and surface-bind into DNA. This conclusion is based upon the effects of hypochromism, the increases in emission intensities and excited-state lifetimes, the helical unwinding, and the excited-state resonance Raman experiment.³¹ The chiral discrimination found in binding these

complexes to DNA lends further support to the intercalative binding model and more specifically to the notion that the binding of this family of rigid complexes with respect to the helix is likely to be quite similar.³² In this series of mixed-ligand complexes, we have varied geometry, hydrophobicity, size, dipole moments, and hydrogen-bonding ability, and we may therefore examine how each of these factors contributes to DNA binding.

Intercalation and Surface Binding. For the mixed-ligand complexes, the tendencies of each of the ligands to intercalate may be compared. For the series $\text{RuX}_2\text{bpy}^{2+}$, $\text{RuX}_2\text{phen}^{2+}$, $\text{RuX}_2\text{DIP}^{2+}$, $\text{RuX}_2\text{phi}^{2+}$, where the ancillary, nonintercalated ligands X are kept constant, the binding constants increase in the series $\text{bpy} \ll \text{phen} \leq \text{DIP} \ll \text{phi}$. This variation likely reflects the differing ability of the ligands to stack and overlap well with the base pairs. The phi ligand is flat, large in surface area, and has a geometry that permits substantial overlap with the base pairs (rather than one where the majority of the π -orbital framework would lie in the center of the helix, between the DNA bases). Hence the phi ligand is well suited for intercalation, and for mixed-ligand complexes it would be the phi ligand that would be expected preferentially to intercalate. The DIP ligand, similar in expanse to that of phi, is not expected to be flat, with phenyl groups instead twisted out of the phenanthroline plane,³³ and this lack of planarity diminishes the favorability of the ligand for intercalation. Nonetheless, the data are consistent with intercalation by this ligand. The DIP ligand, moreover, may be favored over phen for intercalation into the helix. Binding data from absorption titrations for $\text{Ru}(\text{phen})_3^{2+}$ and $\text{Ru}(\text{phen})_2\text{DIP}^{2+}$ show increased binding affinity upon substitution with DIP, and both emission enhancements and red shifts in absorption are greater for analogous DIP versus phen complexes. That this affinity derives from intercalation rather than from added hydrophobic surface binding is not definitively established, however, and therefore the relative intercalative ability of DIP versus phen complexes is difficult to assess. The phen ligand can, nonetheless, also intercalate into the helix, though the ancillary ligands preclude substantial overlap with the base pairs. Inspection of models shows that, owing to the overhanging hydrogen atoms (2- and 3-positions) from the ancillary ligands, only the outer third of the phenanthroline ligand (5- and 6-positions) is available for stacking. Thus only a partial insertion of the ligand is likely. For bpy, this stacking region is absent. On this basis, it is reasonable to understand why the bpy ligand shows only an electrostatic association with DNA, and no detectable intercalation.

Effects of Ancillary Ligands. The primary effect of the ancillary ligand is in altering the extent of enantioselectivity. As was found earlier⁸ in comparisons of $\text{Ru}(\text{phen})_3^{2+}$ and $\text{Ru}(\text{DIP})_3^{2+}$, increased steric bulk of the ancillary ligand increases the enantioselectivity for intercalation of the Δ isomer into right-handed DNA. Given intercalation into the helix by one ligand, we can also compare how different ancillary ligands add to or detract from the overall binding affinity. One bulky hydrophobic ligand that can intercalate adds to the stability of the bound complex, but the second bulky ligand, which would necessarily occupy the ancillary position, perpendicular to the groove, adds no further stability. $\text{Ru}(\text{DIP})_2\text{phen}^{2+}$ shows binding similar to that of $\text{Ru}(\text{phen})_2\text{DIP}^{2+}$, and $\text{Ru}(\text{phi})_2\text{bpy}^{2+}$ actually displays decreased affinity for DNA relative to $\text{Ru}(\text{bpy})_2\text{phi}^{2+}$. For these ancillary ligands, steric interactions may interfere with how deeply the intercalated ligand may stack into the helix. Additionally, the increased hydrophobicity of the complexes leads to self-stacking in solution, and this effect may reduce the net binding affinity.³⁴ Interestingly, symmetric substitutions provide a different picture. In comparing $\text{Ru}(\text{bpy})_2\text{phen}^{2+}$ with $\text{Ru}(\text{phen})_3^{2+}$, or $\text{Ru}(\text{bpy})_2\text{DIP}^{2+}$ with Ru -

(30) Kumar, C. V.; Barton, J. K.; Gould, I. R.; Turro, N. J.; Van Hooten, J. *Inorg. Chem.* **1988**, *27*, 648.

(31) These results taken together provide strong evidence in support of intercalation, but only a crystal structure of the complex bound to the oligonucleotide may be considered definitive.

(32) Although much can be inferred about the binding mode of the complex from these spectroscopic results, conclusions regarding sequence and groove selectivities cannot be drawn. These will require mapping studies with coupled cleavage chemistry.

(33) Goldstein, B. M.; Barton, J. K.; Berman, H. M. *Inorg. Chem.* **1986**, *25*, 842.

(34) The fact that a lower concentration of $\text{Ru}(\text{phi})_2\text{bpy}^{2+}$ is needed for 50% helix unwinding compared to $\text{Ru}(\text{bpy})_2\text{phi}^{2+}$ may be consistent with this idea.

Table III. Characteristics of Complexes

complex	buffer solubility, ^a mM	water-accessible surface area, ^b Å ²
Ru(bpy) ₃ ²⁺	94 (4.4)	687.3
Ru(bpy) ₂ (phen) ²⁺	200 (24.)	702.6
Ru(phen) ₂ (bpy) ²⁺	133 (1.8)	719.6
Ru(phen) ₃ ²⁺	159 (5.3)	736.7
Ru(5-NO ₂ -phen) ₃ ²⁺	28.2 (0.27)	862.6
Ru(phen) ₂ (flone) ²⁺	60 (2.2)	738.9
Ru(bpy) ₂ (DIP) ²⁺	73 (2.5)	916.4
Ru(phen) ₂ (DIP) ²⁺	9 (1.2)	950.2
Ru(DIP) ₂ (phen) ²⁺	0.18 (0.01)	1166.7
Ru(bpy) ₂ (phi) ²⁺	15 (2.0)	768.3
Ru(phen) ₂ (phi) ²⁺	0.17 (0.01)	809.4
Ru(phi) ₂ (bpy) ²⁺	0.018 (0.001)	854.0

^a Measured from saturated solutions in 5 mM Tris, 50 mM NaCl, pH 7.5, after 24 h, 25 °C. Solubilities are given for the chloride salts. Standard deviations are given in parentheses. ^b See ref 36.

(phen)₂DIP²⁺, one finds increased DNA binding affinity with increasing hydrophobicity of the ancillary ligands.³⁵ This observation may in part reflect a greater tendency of phen for surface binding. However, the orientations of the intercalated complexes will certainly affect their ability to exclude water from the hydrophobic surfaces of the ancillary ligands, and this may be particularly important in stabilizing symmetric binding molecules.

Hydrogen Bonding. The series of complexes studied also affords the opportunity to examine whether substitutions of ligands that contain potentially hydrogen-bonding groups stabilize the complexes bound to DNA. Both the red shift in absorption titrations and the finding of enantioselective binding of the Δ isomer suggest that Ru(5-NO₂-phen)₃²⁺ may bind to DNA intercalatively. One might have expected that, with the larger heterocyclic surface of 5-NO₂-phen, the ligand might even have been favored for intercalation. Inspection of models suggests that if intercalated, or indeed even if surface-bound, the nitro groups on the ancillary ligands could be aligned appropriately for hydrogen bonding to base positions. The complex, however, binds only poorly to DNA. In fact that binding constant is comparable to that of Ru(bpy)₃²⁺, and thus the major source of stabilization is likely to be electrostatic. A similar conclusion may be drawn based upon a comparison of binding constants of Ru(phen)₂bpy²⁺ and Ru(phen)₂flone²⁺. For the diazafluorenone ligand, the oxygen atom is oriented perpendicular to the main axis of phenanthroline, and thus the orientation of the hydrogen-bonding acceptor relative to that of either groove containing hydrogen-bonding donors differs from that in Ru(5-NO₂phen)₃²⁺. Yet, again, no increased stabilization is detected. Instead, the binding affinity for Ru(phen)₂flone²⁺ is indistinguishable from that for Ru(phen)₂bpy²⁺. It appears, then, that the substitution of potential hydrogen-bonding acceptors onto the phenanthroline ligands provides no additional source of stabilization. The same observation applies to our single example of a hydrogen-bonding donor on an ancillary ligand, Ru(phi)₂bpy²⁺. For this complex, equilibrium binding constants are in the range of those for Ru(phen)₂phi²⁺. Thus, although specific hydrogen-bonding interactions along the DNA helix are possible, there is apparently no net increase in hydrogen-bonding stabilization relative to that where the DNA and complex are independently solvated. In binding to DNA, some new hydrogen bonds between DNA and complex may be made, but these are at the expense of hydrogen bonds for each with solvent.

Overall Factors Contributing to Stabilization. If one compares the various factors that contribute to stabilizing the metal complexes on the DNA helix, it appears that the most significant factor is that of molecular shape. Those complexes that fit most closely against the DNA helical structure, those in which van der Waals interactions between complex and DNA are maximized, display highest binding affinity. The phi ligand, for example, is

constructed to provide substantial overlap of its aromatic surface with that of the DNA base pairs, and binding constants for those complexes with phi as intercalated ligand show more than 2 orders of magnitude increase in binding affinity. The phi ligand is not well suited as an ancillary ligand, and in fact more stability results from ancillary substitution by DIP rather than by phi. This notion is further exemplified in the differences between symmetrically and nonsymmetrically arranged ancillary ligands, or even more simply in comparisons of binding modes and affinities for phen versus bpy complexes.

Table III summarizes two characteristics of the complexes that may be useful to consider: their solubility in buffer and their water-accessible surface areas.³⁶ Some correlations between these parameters and the intrinsic binding constants of the complexes may be made, and also some deviations are apparent. Certainly the hydrophobicity of a complex appears to be an important criterion in determining binding affinity. Those complexes with more surface area for interaction with DNA and for which interactions with DNA rather than with water are favored display higher overall intrinsic binding constants. Hydrogen-bonding functionalities do not appear to be critical to overall binding stability. Indeed, Ru(5-NO₂-phen)₃²⁺ and Ru(phen)₂flone²⁺ show binding affinities much lower than would be expected on the basis of their solvent-accessible surfaces. Since binding to DNA limits hydrogen-bonding interactions of the free complex with water, the overall free energy change in binding to DNA is reduced by this factor. In contrast, the free energy change in binding to DNA is increased for hydrophobic complexes because of the entropy gain associated with release of water molecules solvating the hydrophobic ligands. Binding affinities for the DIP complexes are, however, not as high as would be expected based upon calculations of accessible surface area, and this is likely because the ligand is not planar. Hydrophobicity is an important factor, but the shape of the complex, the disposition of ligands relative to the helix, and how the ligands fit against the DNA surface appear to be critical for both intercalative and surface-bound interactions.

Shape and hydrophobicity are likely to be important factors governing also the ability of other small molecules to bind to DNA. Similar notions may be important to consider with regard to the binding of proteins to DNA as well. It must be noted, however, that these studies do not directly provide insight into those factors that may govern differential DNA site selectivity. Site-specific DNA cleavage studies using analogous mixed-ligand complexes of rhodium(III) are in progress to address that issue.³⁷

Utility of Transition-Metal Complexes. Coordination chemistry could play a unique role in the development of new compounds that bind site-specifically to biopolymers. Given the structural flexibility and variable dimensionality of transition-metal complexes, one may design and readily prepare a different repertoire of shapes for interaction with DNA than those obtained through organic synthesis alone. Mixed-ligand complexes of ruthenium(II) are particularly well suited to these systematic investigations of recognition. The octahedral transition-metal ion provides the core, in fact a chiral center, for a rigid, well-defined structure of coordinated ligands. The ligands may be varied in a synthetically convenient fashion to produce a family of substitutionally inert DNA binding molecules with a range of ligand functionalities. The intense coloration and rich excited-state properties of the complexes provide a sensitive spectroscopic handle to monitor binding interactions. These and similar complexes may therefore be useful also in studies of recognition of other biopolymers.

Acknowledgment. We are grateful to the National Institutes of Health (Grant GM33309 to J.K.B.), the National Science Foundation, and the Army Office of Research for their generous support of this research. We are also grateful to Dr. F. Arena for his synthesis of [Ru(phen)₂flone]Cl₂ and Dr. H. Gilson for assistance with the nonlinear least-squares calculations.

(35) Consistent with this idea, both Ru(DIP)₃²⁺ and Ru(phi)₃²⁺ appear to bind DNA more avidly than their mixed-ligand analogues, though their poor solubility makes the quantitative comparison difficult.

(36) The calculations of solvent accessible surface area were performed with water as the probe molecule (radius of 1.58 Å) using the program MACROMODEL, written by W. C. Still, Columbia University.

(37) Pyle, A. M.; Long, E. C.; Barton, J. K., submitted for publication.